IOP PUBLISHING
IOP FTC
PLASMA SOURCES SCIENCE AND TECHNOLOGY
Plasma Sources Sci. Technol. **21** (2012) 032001 (5pp)
doi:10.1088/0963-0252/21/3/032001

FAST TRACK COMMUNICATION

Sheath-to-sheath transport of dust particles in a capacitively coupled discharge

Shinya Iwashita[1], Giichiro Uchida[2], Julian Schulze[1], Edmund Schüngel[1], Peter Hartmann[3], Masaharu Shiratani[2], Zoltán Donkó[3] and Uwe Czarnetzki[1]

[1] Institute for Plasma and Atomic Physics, Ruhr University Bochum, 44780 Bochum, Germany
[2] Department of Electronics, Kyushu University, 819-0395 Fukuoka, Japan
[3] Institute for Solid State Physics and Optics, Wigner Research Centre for Physics, Hungarian Academy of Sciences, POB 49, H-1525 Budapest, Hungary

E-mail: shinya.iwashita@rub.de

Received 20 February 2012, in final form 26 March 2012
Published 27 April 2012
Online at stacks.iop.org/PSST/21/032001

Abstract
Transport of micrometer-sized dust particles in a capacitively coupled radio frequency discharge at low pressures of a few Pa is realized experimentally and understood by a kinetic particle simulation combined with a model. Applying a voltage waveform, which consists of two consecutive harmonics with a variable phase angle, θ, to one electrode, control of both the spatial potential profile and the ion density distribution is obtained by adjusting θ. In this way, the electrostatic and ion drag forces, on dust particles initially located at the sheath edge adjacent to the lower electrode, are controlled. The sudden change of θ leads to an abrupt change of the sheath width. This introduces the particles instantaneously into a high potential that accelerates them to high kinetic energies. The experimental results show that a certain minimum change of the discharge symmetry, i.e. of the phase angle, is required to allow the transport of dust particles through the plasma bulk. Beyond this threshold, a part of the transported particles can even be trapped around the edge of the opposing (upper) sheath.

(Some figures may appear in colour only in the online journal)

1. Introduction

The dynamics of dust particles in plasmas is most relevant for fundamental and applied research covering various disciplines; in astrophysics, the dynamics of dust in the interstellar medium is essential for understanding star formation [1]. For fundamental investigations of strongly correlated mesoscopic many-particle systems dust particles can be introduced into low-pressure plasma discharges [2]. In fusion and low-temperature plasma reactors, however, accumulation of dust is a major problem for device operation [3–7]. For optimization of low-temperature discharges used for solar cell manufacturing, e.g. plasma-enhanced chemical vapor deposition of silicon in H_2–SiH_4, methods to manipulate and remove dust clouds to prevent dust coagulation and agglomeration are strongly required. Finally, the bottom-up approach of fabricating novel materials, e.g. microelectronics circuits, medical components and catalysts, is based on an enhanced control of nanoparticles in plasmas [8–11]. Here, we demonstrate a novel method to realize transport control of dust particles in capacitively coupled radio frequency (CCRF) discharges. Similar to previous investigations of phenomena in dusty (complex) plasmas [2, 12–14] micrometer-sized monodisperse dust particles are introduced into the discharge.

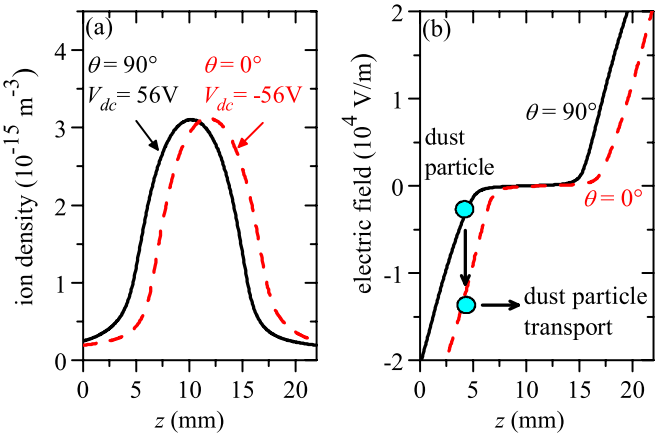

Figure 1. Time-averaged profiles of (a) the ion density and (b) the electric field for $\theta = 90°$ (solid line) and $\theta = 0°$ (dashed line) obtained from PIC/MCC simulations. Discharge conditions: $f = 13.56$ MHz, $\phi_0 = 100$ V, 4 Pa, 22 mm electrode gap.

The particle motion between the electrodes is affected by several forces (electrostatic, thermophoretic, ion and gas drag, and gravitational forces) [15–21]. In reactors with horizontal plane parallel electrodes and in the absence of thermophoretic forces, negatively charged dust particles tend to be confined at the sheath edge near the bottom electrode, where the forces balance. In the presence of a strong thermophoretic force three-dimensional particle clouds, often termed 'Yukawa balls', can be created [22].

The dust manipulation method presented here is based on the electrical asymmetry effect (EAE) [23–25] in CCRF discharges. The EAE allows one to generate and control a dc self-bias, V_{dc}, electrically even in geometrically symmetric discharges. It is based on driving one electrode with a particular voltage waveform, $\phi(t)$, which is the sum of two consecutive harmonics with an adjustable phase shift, θ, between both driving frequencies: $\phi(t) = \phi_0[\cos(2\pi f t + \theta) + \cos(4\pi f t)]$. Here, ϕ_0 is the identical amplitude of both harmonics. In such discharges, V_{dc} is an almost linear function of θ. In this way, separate control of the ion mean energy and flux at both electrodes is realized in an almost ideal way. At low pressures of a few Pa, the EAE additionally allows one to control the maximum sheath voltage and width at each electrode by adjusting θ [23].

The concept of the dust transport method is illustrated in figure 1, which shows the time-averaged ion density and electric field profiles at $\theta = 0°$ and $\theta = 90°$. The data are obtained from a 1D3v particle-in-cell/Monte Carlo collisions (PIC/MCC) simulation of an argon discharge operated at $f = 13.56$ MHz, $p = 4$ Pa, $L = 22$ mm electrode gap and $\phi_0 = 100$ V. For $\theta = 90°$, V_{dc} is maximum and the width of the sheath at the bottom electrode located at $z = 0$ is small. The dust particles find their equilibrium position at the bottom sheath edge, as indicated in figure 1(b). Then, θ is changed abruptly from 90° to 0°. Consequently, a 'new' time-averaged electric field distribution is established on a timescale of microseconds. Due to their high inertia, the dust particles cannot respond to these fast changes. Initially, they stay at their original equilibrium position, which is now located deeper inside the sheath in the new electric field distribution (see figure 1(b)). In this way the dust particles gain a high potential energy and are accelerated toward the upper electrode by the electrostatic force. In the following, this concept and the resulting particle transport will be analyzed and understood experimentally and by a model using input parameters from PIC/MCC simulations.

2. Experimental

The experiments are carried out using a CCRF discharge in argon gas at $p = 4$ Pa, excited by applying $\phi(t)$ with $f = 13.56$ MHz and $\phi_0 = 100$ V. The lower (powered) and upper (grounded) electrodes of 100 mm diameter are placed at a distance of 22 mm. The plasma is confined radially between the electrodes by a glass cylinder, realizing a geometrically almost symmetric discharge configuration. The chamber and the powered electrode are water-cooled to eliminate the influence of the thermophoretic force. The upper electrode has a 20 mm diameter hole at the center sealed with a fine sieve for injecting SiO_2 dust particles of 1.5 μm size, from a dispenser situated above the upper electrode. An aluminum ring (100 mm outer diameter, 60 mm inner diameter, 2 mm height) is set on the lower electrode to confine the dust particles radially. The injected dust particles are observed using the 'two-dimensional laser light scattering' (2DLLS) method [20, 21]. A vertical laser sheet passes between the two electrodes, with height and width of 20 mm and 1 mm, respectively. The laser power is 380 mW at 532 nm. The light scattered by the dust particles is detected through a side window using a CCD camera (equipped with an interference filter and running at a frame rate of 30 pictures per second).

3. Results and discussion

After turning the discharge on and setting θ to 90°, the subsequently introduced dust particles settle near the sheath–bulk boundary at the lower electrode at a height of about 4.8 mm (in time domain I, $t < 0$, see figure 2(b)). Then, an abrupt change in the phase ($\theta = 90° \rightarrow 0°$) is performed at $t = 0$. Following the phase shift, the ion density and the time-averaged electric field profiles change within a few microseconds, as shown in figure 1. Most dust particles are transported upwards into the plasma bulk during a transient state (time domain II). Thereafter, a fraction of the particles reaches the plasma sheath region near the upper electrode and settles there, i.e. sheath-to-sheath transport is realized. The others are transported back towards the sheath adjacent to the lower powered electrode (in time domain III). We observe that a large-enough change in the self-bias voltage is required to transport dust particles through the plasma bulk. The magnitude of this change can be controlled by the magnitude of the phase shift (see figure 2(a)). There is a difference between V_{dc} resulting from the simulation and experiment, i.e. V_{dc} is more negative in the experiment (see figures 1(a) and 2(a)). This difference is caused by the parasitic capacitive coupling between the glass cylinder and the grounded chamber walls [24]. The maximum displacement of dust particles

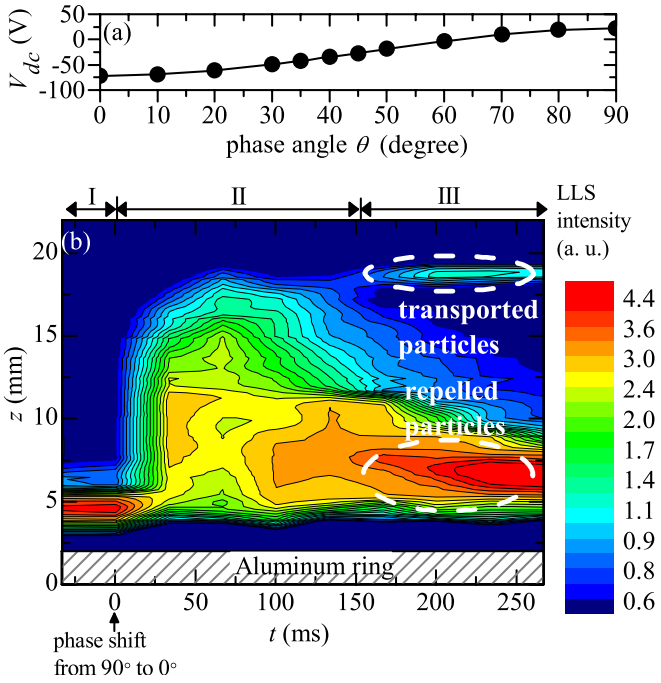

Figure 2. (*a*) The dc self-bias as a function of the phase angle θ. (*b*) Spatiotemporal profile of the LLS intensity from the dust particles between the powered ($z = 0$ mm) and the grounded electrode ($z = 22$ mm). The abrupt phase shift takes place at $t = 0$. Observation of the lower region ($0 \leqslant z \leqslant 2$ mm) is blocked by the aluminum ring.

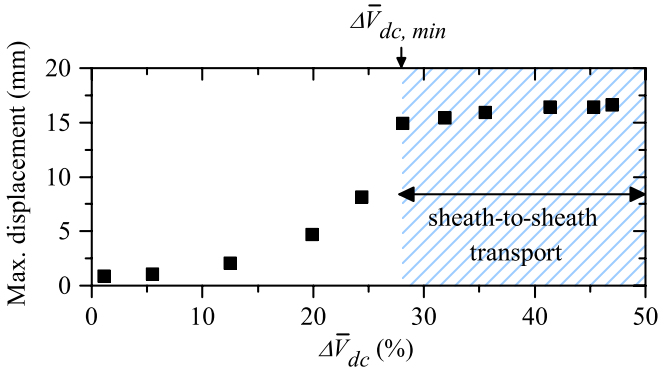

Figure 3. Maximum displacement of dust particles as a function of the normalized $\Delta\bar{V}_{dc}$ induced by an abrupt phase shift. A rather large $\Delta\bar{V}_{dc}$ is required to realize the sheath-to-sheath transport of dust particles.

following the abrupt phase shift is shown in figure 3 as a function of the change in the normalized dc self-bias voltage, $\Delta\bar{V}_{dc} = [V_{dc}(\theta_2) - V_{dc}(\theta_1)]/2\phi_0$. Taking, e.g., $\theta_1 = 90°$, $\theta_2 = 0°$ results in $\Delta\bar{V}_{dc} = 47\%$, and $\theta_2 = 50°$ results in $\Delta\bar{V}_{dc} = 20\%$. The sheath-to-sheath transport is realized at $\Delta\bar{V}_{dc,min} \geqslant 28\%$ at 4 Pa. We observe a strong pressure dependence of $\Delta\bar{V}_{dc,min}$, which may be attributed to gas drag [3, 26].

In order to understand the physical mechanisms that cause the dust transport, we calculate the time-averaged forces acting on the particles, i.e. the ion drag force, F_i, the electrostatic force, F_e, and gravity, F_g, as a function of the position between the electrodes using input parameters from PIC/MCC simulations [27, 28] at $\theta = 0°$ and 90°. There are various models describing F_i [15, 29]. Here, the model of Barnes *et al* [15] is adopted. The ion drag force [5, 15, 16] is calculated according to $F_i = F_{coll} + F_{orb}$, where F_{coll} and F_{orb} are the collection force due to ions hitting the particle surface and the orbit force due to Coulomb collisions with the drifting ions, respectively. The collection force is described as $F_{coll} = n_i v_s m_i v_i \pi b_c^2$. Here n_i, m_i and v_i are the ion density, mass and drift velocity, respectively. The mean ion velocity v_s and the collection impact parameter b_c [15] are

$$v_s = \left(\frac{8k_B T_i}{\pi m_i} + v_i^2\right)^{\frac{1}{2}}, \qquad b_c = r_p\left(1 - \frac{2q\phi_f}{m_i v_s^2}\right)^{\frac{1}{2}}. \quad (1)$$

Here k_B and T_i are the Boltzmann constant and the ion temperature, respectively. r_p, q and ϕ_f are the radius of the dust particles, the elementary charge and the floating potential of the particles relative to the plasma potential, respectively. The orbit force due to Coulomb collisions is given by $F_{orb} = n_i v_s m_i 4\pi b_{\pi/2}^2 \Gamma$, where $b_{\pi/2}$ and Γ are the impact parameter and the Coulomb logarithm:

$$b_{\pi/2} = \frac{q\,Q_p}{4\pi\epsilon_0 m_i v_s^2}, \qquad \Gamma = \frac{1}{2}\ln\left(\frac{\lambda_{De}^2 + b_{\pi/2}^2}{b_c^2 + b_{\pi/2}^2}\right), \quad (2)$$

Q_p, ϵ_0 and λ_{De} are the charge of the dust particles, the vacuum permittivity and the Debye length, respectively. The electrostatic force, F_e, and gravity, F_g, are simply expressed as $F_e = Q_p E$ and $F_g = m_p g$. Here E is the (time-averaged) electric field. The mass of a dust particle m_p is 3.5×10^{-15} kg. In order to calculate these forces, the particle charge is assumed to be constant and estimated to be $Q_p = 1000q$ [5]. This assumption is clearly a simplification in the model, since there is probably some dynamics of the dust charge when exposed to areas of different plasma densities [30]. E, n_i, v_i, ϕ_f, T_i and λ_{De} are taken as input parameters from our simulations. The simulations are performed in pure argon, although PIC/MCC simulations of dusty plasmas have already been reported [31–33]. This approach is based on the assumption that the dust represents only a minor perturbation to the plasma. Due to these simplifications a detailed quantitative agreement of the simulation with the experiment cannot be expected. However, the forthcoming analysis shows that this simplified approach is able to explain the experimental observation of the particle transport qualitatively.

Figure 4 shows the spatial profiles of F_i, F_e and F_g as well as the sum of these forces, F_{tot}, at $\theta = 90°$ and 0°. There are three positions, where the forces balance. The balance point at the center of the plasma bulk, however, corresponds to an unstable equilibrium. Thus, there are only two positions of stable equilibrium at either sheath edge (see figures 4(*b*) and (*d*)), where the particles are observed experimentally. The spatial profiles of the potential energy for each value of θ, derived from the net forces exerted on the dust particles (figure 4), are displayed in figure 5. For each value of θ, there are two local minima of the potential. For $\theta = 0°$, the widths of the corresponding potential wells are L_1 (upper potential minimum) and L_2 (lower potential minimum), respectively.

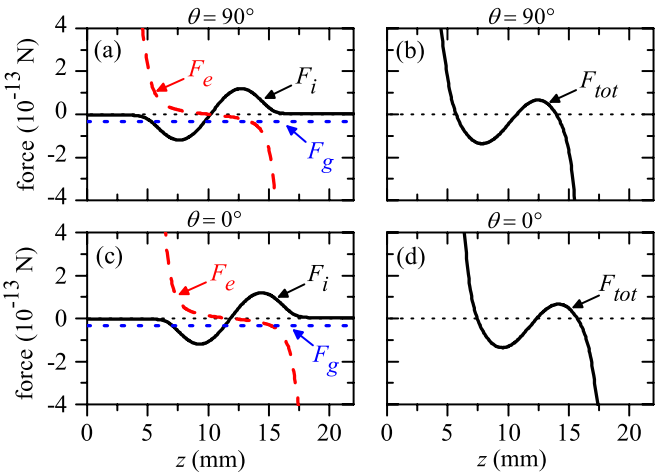

Figure 4. Profiles of the ion drag force, F_i, electrostatic force, F_e, gravity, F_g for $\theta = 90°$ (*a*) and 0° (*c*). The sum of all forces F_{tot} calculated from PIC/MCC simulation data for $\theta = 90°$ and 0° is shown in (*b*) and (*d*).

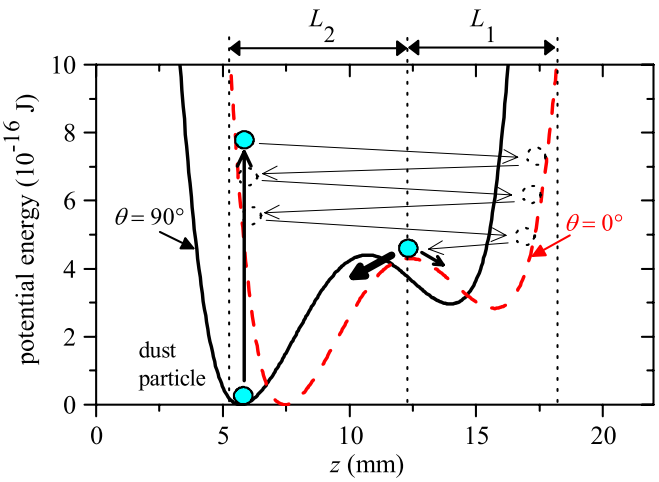

Figure 5. Profiles of the potential energy calculated from PIC/MCC simulation data for $\theta = 0°$ and 90°. The arrows illustrate the particle trajectories and the trapping mechanism.

The values of both potential minima and their widths are different due to the effect of the gravitational force. By changing the phase shift abruptly ($\theta = 90° \rightarrow 0°$), the dust particles initially located at the position of vanishing potential at $\theta = 90°$ close to the bottom electrode are suddenly located in a region of high potential due to their inertia. Consequently, they are transported upwards toward the top electrode. During their transport friction, i.e. the gas drag force, reduces their velocity. The gas drag force is expressed by the collision frequency ν_p for momentum loss between dust particles and gas atoms [34] as $F_f = \nu_p m_p (v_p - v_n)$. Here v_n is the drift velocity of the gas atoms. ν_p is given by

$$\nu_p = \delta \frac{4}{3} \pi r_p^2 \frac{m_n}{m_p} n_n v_{th,n}, \qquad (3)$$

where m_n, n_n and $v_{th,n}$ are the mass of a gas atom, their number density and their thermal velocity, respectively. The coefficient δ is 1 (specular reflection) or $1+8/\pi$ (perfect diffuse reflection) [5, 26, 34]. By estimating the sheath voltage from the applied voltage in the experiment [23] and the position of dust particles from figure 1(*b*), their initial velocity is calculated to be 2.7 m s^{-1}. Because of this large velocity and the high mass ratio of the dust particles compared with the gas atoms, the mean free path of the dust particles is found to be several times as large as the bulk length independent of δ. Therefore, the dust particles bounce between both sheaths several times, while their velocity is reduced due to the gas drag force. Finally, the dust particles, whose kinetic energy is lower than the central maximum of the potential energy in the plasma bulk, are trapped inside the local minimum of the potential profile around either the upper or the lower electrode. The probability of the sheath-to-sheath transport is estimated to be $L_1/(L_1 + L_2) < 0.5$. The position of the lower minimum agrees well between the experiment and the simulation ($z \approx 7.5$ mm; see figures 2 and 5). In the experiment the upper minimum is located at $z = 18.5$ mm, whereas the simulation predicts about 16 mm. This agreement is also reasonable; the differences may be attributed to the possible agglomeration of dust particles, which increases the apparent particle mass. The latter effect makes the potential profile more asymmetric and the upper potential minimum becomes very shallow and narrow, resulting in a small number of dust particles transported toward the upper potential minimum, as shown in figure 2(*b*). The different widths of both potential wells are caused by the effect of gravity. In the limit of high power and ion density, gravity becomes negligible compared with the other forces and the potential profile gets more symmetric for each value of θ. However, then also the energy gain required to overcome the central maximum increases and fewer particles will gain enough energy by the phase kick. In the limit of low power and ion density, the importance of gravity relative to the other forces increases. Then, more particles can be transported to the top electrode, but their chance to be captured in the upper potential well decreases due to the smaller width of this well. Thus, we expect distinct intermediate discharge conditions to realize optimum sheath-to-sheath transport of a large number of dust particles. Alternatively, gravity could be compensated by thermophoretic forces, i.e. by heating the bottom electrode, to make the potential profile more symmetric. Optimizing the sheath-to-sheath transport, however, remains a topic for future investigations outside the scope of this work reporting only the transport mechanisms and its physical causes.

4. Conclusion

We have proposed a novel dust particle transport manipulation method using the electrical asymmetry effect. By changing the phase between two consecutive driving frequencies, the maximum sheath voltage and width at the bottom electrode are changed. In this way the force on the dust particles can be controlled. By abruptly changing the phase from 90° to 0° the dust particles initially located at the sheath edge are strongly accelerated toward the top electrode and can be transported from one sheath to the other. As the mean free path of the microparticles is much longer than the electrode gap, they bounce back and forth between both sheaths, while being

decelerated by collisional friction. Finally, they reside inside the potential well at either the top or the bottom sheath edge. The probability for residing at the top sheath is determined by the width of the upper potential well and, thus, by the relative amplitude of the gravitational force compared with the other forces acting on the dust particles.

Acknowledgments

This research was supported by the German Federal Ministry for the Environment (0325210B), the Alexander von Humboldt Foundation, the RUB Research Department Plasma and the Hungarian Scientific Research Fund (OTKA-K-77653+IN-85261).

References

[1] Ossenkopf V 1993 *Astron. Astrophys.* **280** 617
[2] Bonitz M, Henning C and Block D 2010 *Rep. Prog. Phys.* **73** 066501
[3] Fortov V E, Petrov O F, Molotkov O F, Poustylnik M Y, Torchinsky V M, Khrapak A G and Chernyshevet A V 2004 *Phys. Rev.* E **69** 016402
[4] Shukla P K and Eliasson B 2009 *Rev. Mod. Phys.* **81** 25
[5] Bouchoule A 1999 *Dusty Plasmas* (Chichester: Wiley)
[6] Krasheninnikov S I and Soboleva T K 2005 *Plasma Phys. Control. Fusion* **47** A339
[7] Selwyn G S, Singh J and Bennett R S 1989 *J. Vac. Sci. Technol.* A **7** 2758
[8] Vourdas N, Kontziampasis D, Kokkoris G, Constantoudis V, Goodyear A, Tserepi A, Cooke M and Gogolides E 2010 *Nanotechnology* **21** 085302
[9] Yan H, Choe H S, Nam S W, Hu Y, Das S, Klemic J F, Ellenbogen J C and Lieber C M 2011 *Nature* **470** 240
[10] Kang S K, Seo Y S, Lee H W, Rehman A, Kim G C and Lee J K 2011 *J. Phys. D: Appl. Phys.* **44** 435201
[11] Kim H H, Ogata A, Schiorlin M, Marotta E and Paradisi C 2011 *Catal. Lett.* **141** 277
[12] Thomas H, Morfill G E and Demmel V 1994 *Phys. Rev. Lett.* **73** 652
[13] Chu J H and Lin I 1994 *Phys. Rev. Lett.* **72** 4009
[14] Hayashi Y and Tachibana K 1994 *Japan. J. Appl. Phys.* **33** L804
[15] Barnes M S, Keller J H, Forster J C, O'Neill J A and Coultas D K 1992 *Phys. Rev. Lett.* **68** 313
[16] Zafiu C, Melzer A and Piel A 2003 *Phys. Plasmas* **10** 1278
[17] Rothermel H, Hagl T, Morfill G E, Thoma M H and Thomas H M 2002 *Phys. Rev. Lett.* **89** 175001
[18] Maurer H, Basner R and Kersten H 2008 *Rev. Sci. Instrum.* **79** 093508
[19] Liu B, Goree J, Fortov V E, Lipaev A, Molotkov V I, Petrov O F, Morfill G E, Thomas H M and Ivlev A V 2010 *Phys. Plasmas* **17** 053701
[20] Koga K, Iwashita S and Shiratani M 2007 *J. Phys. D: Appl. Phys.* **40** 2267
[21] Shiratani M, Koga K, Iwashita S and Nunomura S 2008 *Faraday Discuss.* **137** 127
[22] Arp O, Block D and Piel A 2004 *Phys. Rev. Lett.* **93** 165004
[23] Heil B G, Czarnetzki U, Brinkmann R P and Mussenbrock T 2008 *J. Phys. D: Appl. Phys.* **41** 165202
[24] Schulze J, Schüngel E and Czarnetzki U 2009 *J. Phys. D: Appl. Phys.* **42** 092005
[25] Schüngel E, Zhang Q Z, Iwashita S, Schulze J, Hou L J, Wang Y N and Czarnetzki U 2011 *J. Phys. D: Appl. Phys.* **44** 285205
[26] Epstein P S 1924 *Phys. Rev.* **23** 710
[27] Donkó Z, Schulze J, Czarnetzki U and Luggenhölscher D 2009 *Appl. Phys. Lett.* **94** 131501
[28] Donkó Z 2011 *Plasma Sources Sci. Technol.* **20** 024001
[29] Fortov V E and Morfill G E 2009 *Complex and Dusty Plasmas* (Boca Raton, FL: CRC Press)
[30] Hübner S and Melzer A 2009 *Phys. Rev. Lett.* **102** 215001
[31] Choi J S, Ventzek P L G, Hoekstra R J and Kushner M J 1994 *Plasma Sources Sci. Technol.* **3** 418
[32] Schweigert I V, Alexandrov A L, Ariskin D A, Peeters F M, Stefanović V, Kovačević E, Berndt J and Winter J 2008 *Phys. Rev.* E **78** 026410
[33] Matyash K, Schneider R, Taccogna F, Hatayama A, Longo S, Capitelli M, Tskhakaya D and Bronold F X 2007 *Contrib. Plasma Phys.* **47** 595
[34] Piel A 2010 *Plasma Physics* (Berlin: Springer)